



# Reverse Engineering Field Isolates of Myxoma Virus Demonstrates that Some Gene Disruptions or Losses of Function Do Not Explain Virulence Changes Observed in the Field

June Liu,<sup>a</sup> Isabella M. Cattadori,<sup>b</sup> Derek G. Sim,<sup>b</sup> John-Sebastian Eden,<sup>c,d</sup>  
Edward C. Holmes,<sup>c</sup> Andrew F. Read,<sup>b,e</sup> Peter J. Kerr<sup>a,c</sup>

CSIRO Health and Biosecurity, Black Mountain Laboratories, Acton, ACT, Australia<sup>a</sup>; Center for Infectious Disease Dynamics, Department of Biology, The Pennsylvania State University, University Park, Pennsylvania, USA<sup>b</sup>; Marie Bashir Institute for Infectious Diseases and Biosecurity, Charles Perkins Centre, School of Life and Environmental Sciences, University of Sydney, Sydney, NSW, Australia<sup>c</sup>; Centre for Virus Research, The Westmead Institute for Medical Research, Sydney, Australia<sup>d</sup>; Department of Entomology, The Pennsylvania State University, University Park, Pennsylvania, USA<sup>e</sup>

**ABSTRACT** The coevolution of myxoma virus (MYXV) and wild European rabbits in Australia and Europe is a paradigm for the evolution of a pathogen in a new host species. Genomic analyses have identified the mutations that have characterized this evolutionary process, but defining causal mutations in the pathways from virulence to attenuation and back to virulence has not been possible. Using reverse genetics, we examined the roles of six selected mutations found in Australian field isolates of MYXV that fall in known or potential virulence genes. Several of these mutations occurred in genes previously identified as virulence genes in whole-gene knockout studies. Strikingly, no single or double mutation among the mutations tested had an appreciable impact on virulence. This suggests either that virulence evolution was defined by amino acid changes other than those analyzed here or that combinations of multiple mutations, possibly involving epistatic interactions or noncoding sequences, have been critical in the ongoing evolution of MYXV virulence. In sum, our results show that single-gene knockout studies of a progenitor virus can have little power to predict the impact of individual mutations seen in the field. The genetic determinants responsible for this canonical case of virulence evolution remain to be determined.

**IMPORTANCE** The species jump of myxoma virus (MYXV) from the South American tapeti to the European rabbit populations of Australia and Europe is a canonical example of host-pathogen coevolution. Detailed molecular studies have identified multiple genes in MYXV that are critical for virulence, and genome sequencing has revealed the evolutionary history of MYXV in Australia and Europe. However, it has not been possible to categorically identify the key mutations responsible for the attenuation of or reversion to virulence during this evolutionary process. Here we use reverse genetics to examine the role of mutations in viruses isolated early and late in the Australian radiation of MYXV. Surprisingly, none of the candidate mutations that we identified as likely having roles in attenuation proved to be important for virulence. This indicates that considerable caution is warranted when interpreting the possible role of individual mutations during virulence evolution.

**KEYWORDS** myxoma virus, virulence, gene disruption, reverse genetics, rabbits, evolution

Received 27 July 2017 Accepted 27 July 2017  
Accepted manuscript posted online 2 August 2017

**Citation** Liu J, Cattadori IM, Sim DG, Eden J-S, Holmes EC, Read AF, Kerr PJ. 2017. Reverse engineering field isolates of myxoma virus demonstrates that some gene disruptions or losses of function do not explain virulence changes observed in the field. *J Virol* 91:e01289-17. <https://doi.org/10.1128/JVI.01289-17>.

**Editor** Rozanne M. Sandri-Goldin, University of California, Irvine

**Copyright** © 2017 American Society for Microbiology. All Rights Reserved.

Address correspondence to Edward C. Holmes, [edward.holmes@sydney.edu.au](mailto:edward.holmes@sydney.edu.au), or Peter J. Kerr, [pjker104@gmail.com](mailto:pjker104@gmail.com).

**TABLE 1** Virulence grades<sup>a</sup>

Grade	CFR (%)	AST (days)
1	>99	≤13
2	95–99	14–16
3A	90–95	17–22
3B	70–90	23–28
4	50–70	29–50
5	<50	NA

<sup>a</sup>Based on data reported previously (19). NA, not applicable.

Viruses that jump species boundaries are a major cause of emerging infectious diseases in humans and other animals. Successful cross-species transmission events are usually associated with the accumulation of mutations across the virus genome, although determining their exact role in host adaptation is complex (1–4). When emerging diseases present with extremely high virulence in the new host, there can be strong selection for attenuation. This is because rapid host death can compromise transmission, so less-lethal pathogen strains may have a fitness advantage. There has been considerable discussion and some experimentation on what level of virulence maximizes transmission under different conditions (5–12).

From this perspective, the release of myxoma virus (MYXV) as a biological control agent for wild European rabbits (*Oryctolagus cuniculus*) in Australia in 1950 started a remarkable natural evolutionary experiment. This continent-scale experiment was replicated in Europe in 1952 with the release and establishment of a separate strain of MYXV (13). Strikingly, the results of the two real-world experiments were similar: moderately attenuated viruses replaced the initial highly lethal viruses in the field, and rabbits with resistance to myxomatosis were selected in the wild population (13, 14).

This coevolution of MYXV and European rabbits has become a textbook model of the arms race between pathogens and hosts (5, 11, 14, 15). In its native host, the South American tapeti (*Sylvilagus brasiliensis*), MYXV causes a relatively innocuous, localized cutaneous fibroma. However, in European rabbits, the same virus overwhelms host defenses and spreads systemically, causing the lethal disease myxomatosis. Case fatality rates (CFRs) caused by the viruses initially released in Australia and Europe were >99% (16).

MYXV is passively transmitted by biting arthropods such as mosquitoes and fleas, which pick up the virus on their mouthparts while probing through virus-rich cutaneous lesions. Moderately attenuated viruses had an advantage over the initial highly lethal viruses because infected rabbits survived longer in an infectious state. However, highly attenuated viruses were poorly transmitted because high titers of virus were present in cutaneous tissues only transiently (17).

In early studies of the evolution of MYXV, viruses isolated from the field in Australia and Europe were categorized into five (and later six) virulence grades. These grades were assigned on the basis of the CFR and average survival time (AST) of a small group of (usually five) laboratory rabbits infected with each isolate (Table 1). Grade 1 viruses were lethal, with a CFR of ~100% and an AST of <13 days, while grade 5 viruses had CFRs of <50%. Grade 3 viruses, with CFRs of 70 to 90%, as measured in unselected laboratory rabbits, came to predominate in the field (14, 18–20), although grade 4 viruses, with CFRs of 50 to 70%, were the viruses most transmissible by mosquitoes in experimental studies of laboratory rabbits (17). This suggests that the emergence of resistance in wild rabbits meant that higher-virulence grade 3 viruses were more successful in the field since they were effectively of lower virulence in resistant rabbits (21–24). It is also likely that ongoing selection for resistance in the rabbit population may be continuing to select for viruses of higher virulence when tested in unselected laboratory rabbits.

Two unusual features of the MYXV-rabbit coevolution model are that we have the original viruses used to initiate the epidemics in Australia and Europe and that laboratory rabbits are the same species as wild European rabbits and develop an

**TABLE 2** Mutations in target genes<sup>a</sup>

Target gene	Virus	Protein function(s)	Mutation(s)
<i>M005L/R</i>	SLS; Ur	E3 ubiquitin ligase, host range factor, antiapoptosis	<i>M005L/R</i> ORF is disrupted in SLS (C insert) and Ur (CC insert) after nt 34; an alternative ATG codon at positions 17–19 can potentially correct the ORF of SLS but not of Ur
<i>M012L</i>	OB3 Y317	dUTPase (dephosphorylation of dUTP to dUMP to minimize its incorporation into DNA)	Deletion of 13 nt (nt 175–187) in <i>M012L</i> ; <i>M012</i> (148 aa) sequence is truncated at aa 70; normal protein is a homotrimer
<i>M014L</i>	Ur	Putative E3 ubiquitin ligase with N-terminal BTB-BACK domain and C-terminal Kelch domains	C insert at nt 1406; <i>M014</i> (517 aa) is truncated after aa 478 with loss of a C-terminal Kelch domain
<i>M153R</i>	Meby	E3 ubiquitin ligase; reduces the cell surface expression of MHC-I and CD4	73-nt deletion (nt 508–580); <i>M153</i> (206 aa) is changed after residue 169, replacing the CR essential for MHC-I downregulation with a novel sequence from a new ORF, leading to a predicted protein of 211 aa
<i>M153R</i>	OB3 Y317	E3 ubiquitin ligase; reduces the cell surface expression of MHC-I and CD4	Substitution E177A in <i>M153</i>
<i>M156R</i>	WS6 1071	eIF2 $\alpha$ homologue binds PKR and inhibits IFN-induced shutdown of protein synthesis	Substitution L98P prevents inhibition of PKR

<sup>a</sup>Shading indicates genes that have been implicated in virulence. IFN, interferon.

essentially identical disease when infected with MYXV (18). Thus, laboratory rabbits serve as an unselected host to compare viruses from the field with the progenitor viruses in a naturally evolving system.

MYXV belongs to the *Leporipoxvirus* genus of the family *Poxviridae* (subfamily *Chordopoxvirinae*). The sequence of the MYXV strain originally released in Europe (Brazil/Campinas/1949), known as the Lausanne (Lu) strain, has become the reference genome and consists of 161 kb of linear double-stranded DNA (dsDNA) with terminal inverted repeats (TIRs) of 11.5 kb at both ends and closed single-strand hairpin loops at each end. It is predicted to harbor 158 unique open reading frames (ORFs), 12 of which are duplicated in the TIR (25, 26). The genome sequences of multiple MYXV strains isolated from wild rabbits in Australia and Europe, including the Australian progenitor virus (Brazil/1910), termed the standard laboratory strain (SLS), have now been determined (27, 28). However, attempts to correlate sequence changes with virus phenotypes have been complicated both by the number of different mutations observed and because none of these mutations appeared to be uniquely correlated with either the attenuation of or reversion to virulence (27, 28). Therefore, the molecular mechanisms underlying the virulence evolution of MYXV in wild-rabbit populations between the 1950s and 1990s remain unknown.

We aimed to understand the roles of specific mutations in the initial attenuation and potential reversion to virulence in the field. Single-gene knockout studies have been extensively used to examine the function of genes in MYXV with the Lu strain or the Lu-derived T1 strain, and most reported studies demonstrated a reduction, often dramatic, in virulence, as measured by CFRs, when the virus was tested in laboratory rabbits (29). However, no reverse-genetics approach has been performed with wild-type Australian isolates to determine the genetic basis of this canonical case of virulence evolution in the field.

We reverse engineered six candidate mutations (Table 2) that were present in Australian MYXV isolates early or late in the radiation of the progenitor SLS from 1950 (Table 3). Three of the four isolates that we genetically manipulated were attenuated compared to their highly virulent progenitor, and we anticipated that reversing the mutations would restore or increase virulence. In the remaining case, we inserted a mutation predicted to decrease virulence into a virulent isolate.

The first of the attenuated viruses, the Australia/Uriarra/1953 (Ur) strain, was isolated in 1953, only 2 years after the spread of SLS with grade 1 virulence in Australia. Ur was the first highly attenuated virus characterized in detail (30) and differs from SLS by only 8 nucleotide (nt) substitutions and 5 single-nucleotide indels, 2 of which are intergenic (27). The short genetic distance from SLS and its significant attenuation made Ur an

**TABLE 3** Summary of mutations<sup>a</sup> present in viruses selected for reverse engineering compared to the SLS progenitor

Virus (yr isolated; virulence grade)	No. of synonymous substitutions	No. of nonsynonymous substitutions	Indels in ORFs	No. of intergenic indels <sup>b</sup>	No. of intergenic substitutions
Ur (1953; 5 <sup>b</sup> )	3	5	<u>M005L/R</u> , <sup>c</sup> <u>M014L</u> , <u>M134R</u> <sup>d</sup>	2	0
Meby (1991; 3/4)	24	35	<u>M009L</u> , <sup>e</sup> <u>M083L</u> , <sup>f</sup> <u>M134R</u> , <b>M153R</b>	3	1
SWH 8/2/93 (1993; 2)	21	40	<u>M009L</u> , <u>M083L</u> , <u>M134R</u>	10	1
OB3 Y317 (1994; 5)	24	42	<u>M009L</u> , <b><u>M012L</u></b> , <u>M021L</u> , <sup>g</sup> <u>M018L</u> , <u>M064R</u> , <u>M083L</u> , <u>M134R</u> , <u>M156R</u>	9	1

<sup>a</sup>Mutations in TIRs were counted only once.

<sup>b</sup>Ur was originally defined as the prototype grade 4 virulence virus (18), but in our hands, it has consistently been a grade 5 virus causing severe clinical myxomatosis but a very low CFR.

<sup>c</sup>Genes in boldface type were replaced in reverse-engineered viruses and are described in Table 1. Underlined genes have the reading frame disrupted.

<sup>d</sup>Ur has a single A insert toward the 3' end of *M134L*. This disrupts the ORF and leads to a protein that retains a predicted C-terminal transmembrane domain but is 27 aa shorter than the 2,000-aa SLS protein. All the other viruses have a 3A insert at this point, which maintains the ORF.

<sup>e</sup>*M009L* is disrupted in all but one Australian virus isolate made after 1990; M009 is predicted to be an E3 ubiquitin ligase.

<sup>f</sup>The insertion in *M083L* repairs a disrupted ORF found in SLS and early-derived viruses such as Ur.

<sup>g</sup>Insertions in *M021L* and *M064R* do not disrupt the ORF. The insertion in *M018L* alters the sequence after aa 60 and reads through to add an extra 20 aa to the normal 66-aa sequence. The function of this protein is not known. The indel in *M156R* is at the 3' end of the gene and leads to a readthrough with the addition of 2 aa at the C terminus of the protein. M156 is an eIF2 $\alpha$  homologue that inhibits protein kinase R.

<sup>h</sup>Intergenic indels range in size from 1 to 32 nt.

attractive target for proof-of-concept reverse-genetics studies to determine the mechanism of attenuation.

In addition, we reversed gene disruptions in two attenuated viruses isolated in Australia in the 1990s, Australia/Meby/1991 (Meby) (grade 3/4 virulence) and Australia/OB3/Y317/1994 (OB3 Y317) (grade 5 virulence). We also inserted a candidate attenuation mutation into a virulent isolate, Australia/SWH/8-2-93/1993 (SWH 8/2/93) (grade 2 virulence).

In total, we tested six mutations in five genes for their impacts on virulence (Tables 2 to 4). The rationale for testing these candidates was as follows. (i) A single-nucleotide insertion near the 5' end of *M005L/R* occurs in the Australian progenitor SLS virus and in all subsequent Australian isolates sequenced to date (27, 28). When *M005L/R* was knocked out in Lu, CFRs were reduced from 100% to 0% (31). Because of this apparently critical role in virulence, we previously speculated that an alternate ATG codon is used to initiate the *M005L/R* reading frame in SLS (27). However, in Ur, there are 2 nt inserted, and this alternate ATG codon cannot correct the ORF. Thus, *M005L/R* contains one of the few genetic differences between the highly attenuated Ur strain and its virulent progenitor SLS. In addition, the mutation in *M005L/R* in SLS is a potential explanation for the lower virulence of SLS than of Lu when the viruses are compared in genetically resistant rabbits (14). (ii) The indel disrupting *M014L* is another of the few genetic differences between Ur and SLS. Although we considered it unlikely to be significant in attenuation, since the same mutation is found in more-virulent viruses (27), we con-

**TABLE 4** Reverse-engineered viruses produced in this study<sup>a</sup>

Parental virus	Reverse-engineered virus	Inserted gene(s)
Ur	Ur-Lu-M005	Lu <i>M005L/R</i>
Ur	Ur-SLS-M005	SLS <i>M005L/R</i>
Ur	Ur-Ur-M005	Ur <i>M005L/R</i>
Ur	Ur-SLS-M014	SLS <i>M014L</i>
Ur	Ur-Ur-M014	Ur <i>M014L</i>
Ur-SLS-M014	Ur-SLS-M014-Lu-M005	SLS <i>M014L</i> , Lu <i>M005L/R</i>
OB3 Y317	OB3-BRK-M012	BRK 897 <i>M012L</i>
OB3 Y317	OB3-OB3-M012	OB3 Y317 <i>M012L</i>
OB3-BRK-M012	OB3-BRK-M012-SWH/9/92-M153	SWH 9/92 <i>M153R</i>
Meby	Meby-SWH/9/92-M153	SWH 9/92 <i>M153R</i>
Meby	Meby-Meby-M153	Meby <i>M153R</i>
SWH 8/2/93	SWH/8/2/93-WS6-M156	WS6 1071 <i>M156R</i>
SWH 8/2/93	SWH8/2/93-SWH8/2/93-M156	SWH 8/2/93 <i>M156R</i>

<sup>a</sup>Shading indicates revertant control viruses.

**TABLE 5** Additional mutations found in the reverse-engineered viruses compared to the parental viruses

Mutation (position <sup>a</sup> )	Consequence of mutation	Reverse-engineered virus(es)
A insert (131598)	Already an A insert at this point in <i>M134R</i> disrupting the ORF	Ur-Lu-M005, Ur-SLS-M005, Ur-Ur-M005
A insert (122726)	Reads through the stop codon and changes the last 3 amino acids of M130 (undefined immunosuppressive function)	Ur-SLS-M005
T>C (11047)	Synonymous mutation in <i>M008.1L/R</i>	OB3-OB3-M012
C>T (58767)	Synonymous mutation in <i>M062R</i>	OB3-OB3-M012
A insert (16617) <sup>b</sup>	Intergenic	Ur-SLS-M014, Ur-SLS-M014-Lu-M005
T>C (14485)	D34G in M012 (dUTPase)	Ur-Ur-M014
T>C (79660)	Y121H in M081 (early transcription factor subunit)	Meby-SWH/9/92-M153, Meby-Meby-M153
C>T (38180)	S333N in M036 (signal transduction enhancement in VACV)	Meby-SWH/9/92-M153
T insert (149087) <sup>b</sup>	Intergenic	Meby-SWH/9/92-M153
A>G (11458) <sup>b</sup>	Intergenic	SWH8/2/93-WS6-M156
T deletion (149225)	Intergenic	SWH8/2/93-SWH8/2/93-M156

<sup>a</sup>The position is based on the sequence of the parental virus strain in each group.

<sup>b</sup>Mutations were knowingly introduced because the flanking sequence of the inserted genes differed from the original sequence at this point.

sidered it important to test the result of repairing the mutation and to also test the result of repairing both the *M005L/R* and *M014L* genes together in the Ur background. (iii) A 13-nt deletion disrupts the *M012L* gene in OB3 Y317, the most attenuated field isolate that we have seen from Australia. Although there was no information on any role for *M012L* in virulence of MYXV, we considered it the most likely mutation to explain attenuation. (iv) *M153R* is disrupted by a 73-bp deletion in the attenuated Meby isolate (27). When *M153R* was knocked out in the Lu-derived T1 strain, case fatality rates were reduced from 100% to 30% (32). We replaced the Meby *M153R* gene with an intact copy since this seemed the most likely explanation for attenuation. We also tested the possible role of a glutamate-to-alanine amino acid substitution in *M153R* found in the highly attenuated OB3 Y317 virus. (v) A single-amino-acid substitution, L98P, in the protein encoded by *M156R* causes a loss of function by abrogating the inhibition of protein kinase R (PKR), and it has been suggested that this may have been critical for the attenuation of Australian viruses (33). This substitution occurs independently on two branches of the Australian phylogeny (28); however, its role in virulence in rabbits has not been assessed. We therefore tested this by inserting *M156R* encoding P98 into a virulent virus (grade 2).

## RESULTS

**Reverse-engineered viruses.** For each of the mutations selected for reverse engineering, we first replaced the MYXV gene in the parental virus with the mCherry fluorescent marker gene (knockout virus) and then replaced the marker gene with either the original MYXV gene from the parental virus to re-create the parental virus (revertant control virus) or a replacement copy of the MYXV gene without the mutation (knock-in virus). We made a total of 13 reverse-engineered viruses, including 5 revertant control viruses and 2 viruses which had two candidate mutations reversed (Table 4; see also Fig. S1 in the supplemental material).

**Genome sequencing of reverse-engineered viruses.** All gene sequences inserted during reverse engineering were confirmed by Sanger sequencing of the reverse-engineered viruses. In addition, to determine whether any other mutations had occurred, we sequenced the entire genomes of all the reverse-engineered viruses (Table 5). This revealed that one mutation (an A insert in *M134R*) was selected in the original Ur-M005 knockout virus because it is present in all three reverse-engineered viruses in the Ur-M005 group. This does not alter the amino acid sequence of Ur M134 because an A insert at the same position in Ur *M134R* already disrupted the ORF. Hence, it likely reflects plaque purification of a subpopulation within the virus stock (28). Similarly, the T>C substitution in Meby *M081L* must have occurred in the Meby-M153 knockout virus, as this substitution is present in both knock-in viruses in the Meby-M153 group. There are nine other such mutations in different virus constructs, including four in intergenic regions and two that are synonymous. The mutations in *M012L*, *M036L*, and *M130R* were considered unlikely to be significant, and these reverse-engineered viruses indeed

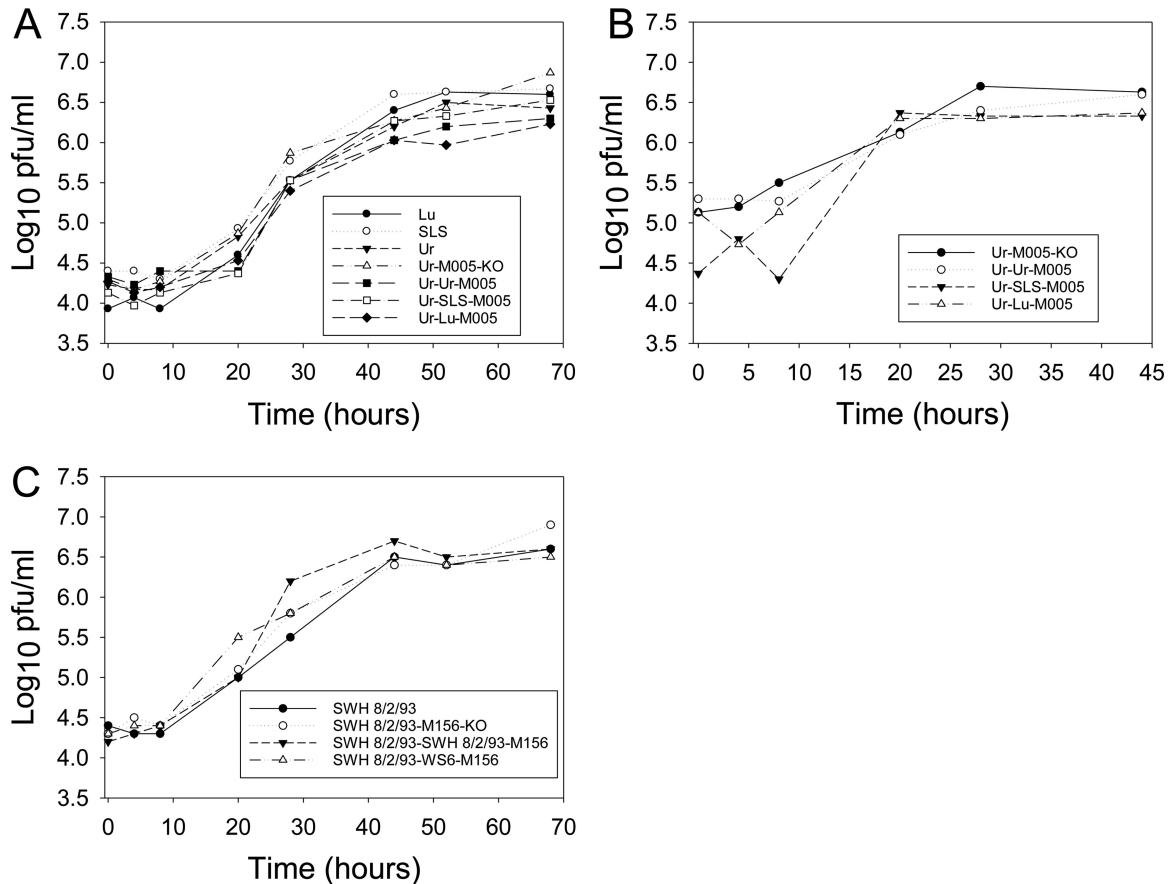


**FIG 1** Replication of reverse-engineered and knockout (KO) viruses in RL-5 T lymphocytes. (A) Growth curves of Ur, SLS, Lu, and Ur with *M005L/R* knocked out or replaced with *M005L/R* from Ur, SLS, or Lu at an MOI of 0.05. (B) Single-step growth curves of Ur with *M005L/R* knocked out or replaced with *M005L/R* from Ur, SLS, or Lu at an MOI of 5 in RL-5 cells. (C) Growth curves of SWH 8/2/93 with *M156R* knocked out or replaced with *M156R* from SWH 8/2/93 or WS6/1071 at an MOI of 0.05. Each growth analysis was performed in triplicate, and the geometric means for each time point are shown.

did not show phenotypic changes compared with the parental viruses. In the case of the *M130R* mutation, it was present only in the Ur-SLS-M005 virus, and the Ur-Lu-M005 virus acts as a control for this mutation. None of the mutations were located in predicted promoter sequences.

An intergenic substitution was knowingly introduced in the left-hand (LH) TIR when *M156R* with the L98P substitution was inserted, since this gene overlaps the TIR boundary at the right-hand (RH) end of the genome; therefore, the sequence is partially duplicated (but noncoding) in the LH TIR, and another intergenic mutation was knowingly introduced with the flanking sequence of Australia/SWH/9-1992 (SWH 9/92) *M153R*, as this sequence differed from the Meby sequence at this point.

**Comparison of the phenotypes of reverse-engineered viruses in cell culture.** All of the knockout viruses replicated normally in RK13 cells during the virus construction phase. Thus, *M005L/R*, *M014L*, *M012L*, *M153R*, and *M156R* were not essential for replication in RK13 cells. However, *M005L/R* has been shown to be essential for replication in primary rabbit lymphocytes and in the rabbit CD4<sup>+</sup> T cell line RL-5, and replication in lymphocytes has been implicated in virulence (31). We compared the replication of the viruses reverse engineered with *M005L/R* to those of the *M005L/R* knockout virus together with the parental Ur, SLS, and Lu viruses in RL-5 cells. There was no difference in virus replication during multistep growth in RL-5 cells (Fig. 1A) or during single-step growth with the Ur-M005 knockout virus and the three Ur-M005 reverse-engineered viruses (Fig. 1B). In addition, to test whether there was any cell permissivity associated with *M156*, we measured the replication of the *M156* reverse-engineered viruses and



**TABLE 6** Reverse-engineered virus phenotypes in rabbits

Virus	Clinical phenotype	CFR (no. of surviving rabbits/ total no. of rabbits tested) (estimated virulence grade; AST [days]) <sup>a</sup>
Ur-SLS-M005	Cutaneous/moderately severe	0/6 (5)
Ur-Lu-M005	Cutaneous/severe	0/6 (5)
Ur-Ur-M005	Cutaneous/severe	0/6 (5)
Ur-SLS-M014	Cutaneous/severe	0/6 (5)
Ur-Ur-M014	Cutaneous/severe	0/6 (5)
Ur-SLS-M014-Lu-M005 <sup>b</sup>	Cutaneous/mild	0/6 (5)
OB3-BRK-M012	Cutaneous/mild	0/6 (5)
OB3-OB3-M012	Cutaneous/mild	0/6 (5)
OB3-BRK-M012-SWH9/92-M153 <sup>b</sup>	Cutaneous/mild	0/6 (5)
Meby-SWH/9/92-M153	Cutaneous/severe <sup>c</sup>	3/6 (4; 26)
Meby-Meby-M153	Cutaneous/severe	4/6 (3; 16)
SWH 8/2/93-WS6-M156	Amyxomatous; acute death	6/6 (2; 13.5)
SWH 8/2/93-SWH 8/2/93-M156	Amyxomatous; acute death	6/6 (2; 14.2)

<sup>a</sup>The AST (average survival time) (in days) is calculated from the ST normalized as  $\log_{10}(ST - 8)$  and then back-transformed; rabbits alive at the end of the trial were assigned an ST of 60 days (18); virulence grades were assigned as described previously (18, 19). Where all rabbits survived, no AST is shown.

<sup>b</sup>Virus tested in rabbits sourced from Charles River Laboratories.

<sup>c</sup>One rabbit had only very mild disease of a short duration; the exclusion of this rabbit would reduce the AST to 23 days.

the *M156R* knockout in RL-5 cells and again observed no differences in replication (Fig. 1C). Others have demonstrated attenuated replication of the Lu strain of MYXV with the M156 L98P mutation in an *M029L*-negative background in RK13 cells (33). In our experiments, all viruses had an intact *M029L* gene, which is also an inhibitor of PKR (34).

**Phenotypes of reverse-engineered viruses in laboratory rabbits.** The clinical phenotype of each virus was assessed by infection of groups of six laboratory rabbits. Clinical assessments of disease signs and severity were made on a qualitative and semiquantitative basis. Virulence was estimated by using survival times (STs) and CFRs, as shown in Table 1, and STs were compared by using Kaplan-Meier plots.

**Ur-M005 reverse-engineered viruses.** We predicted that the replacement of Ur *M005L/R* with the SLS or Lu *M005L/R* gene would lead to a stepwise increase in virulence over that of the revertant control. Notably, however, there was little difference among the three viruses.

In each group, rabbits developed typical nodular cutaneous myxomatosis characterized by a large, fleshy, raised primary lesion at the inoculation site; swollen heads; swollen, partially closed eyelids, sometimes becoming thickened and granular; swelling at the base of the ears; mild to moderate anogenital swelling; and secondary raised cutaneous lesions over the body, ears, and legs (Table 6). As is typical of infections with attenuated MYXV strains, there was a wide range of clinical severity within and between the groups of rabbits (18). Subjectively, it appeared that the rabbits infected with the Ur-SLS-M005 virus had somewhat milder clinical signs than did rabbits in the other two groups; however, no rabbits died or were euthanized in any of the 3 groups prior to the termination of the trial at day 25. The similarity between clinical outcomes can be seen in the temperature plots for each group, with an increase in temperature to  $>40^{\circ}\text{C}$  at around days 5 to 8 and then a return toward normal temperatures ( $38.5^{\circ}\text{C}$  to  $39.9^{\circ}\text{C}$ ) and with some rabbits continuing to have chronically elevated temperatures (Fig. 2A to C).

**Ur-M014 reverse-engineered viruses.** There are no data on the role of M014 in virulence. Here, rabbits infected with the Ur-SLS-M014 virus had clinical signs indistinguishable from those of rabbits infected with the Ur-Ur-M014 revertant virus and essentially identical to those described above for rabbits infected with the Ur-M005 viruses (Table 6 and Fig. 2D and E).

**Ur-M005-M014 double-reverse-engineered virus.** The double-reverse-engineered virus Ur-Lu-M005-SLS-M014 caused only relatively minor disease (Table 6 and Fig. 2F).

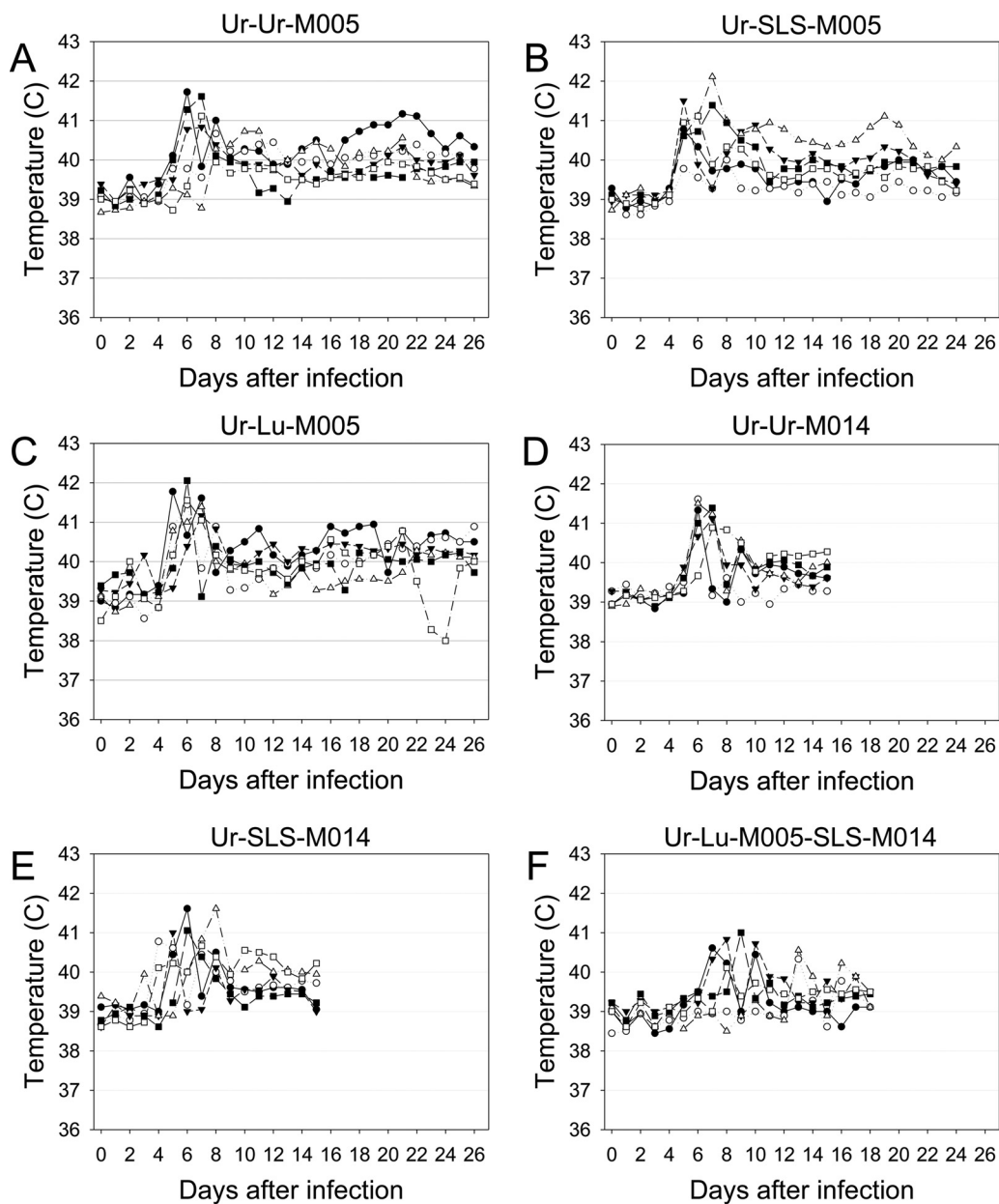


**FIG 2** Daily rectal temperatures of rabbits infected with the reverse-engineered Ur viruses. (A) Ur-Ur-M005; (B) Ur-SLS-M005; (C) Ur-Lu-M005; (D) Ur-Ur-M014; (E) Ur-SLS-M014; (F) Ur-Lu-M005-SLS-M014.

Thus, the reversal of the disruptions in *M005L/R*, *M014L*, or the combination of the two genes did not significantly alter the virulence or clinical phenotype of Ur.

**OB3 Y317-M012 reverse-engineered viruses.** The extreme attenuation of OB3 Y317 was not matched by the loss of defined virulence genes. As such, the disrupted *M012L* gene stood out as a possible explanation for attenuation. However, rabbits infected with either OB3-BRK-M012 or the revertant virus had indistinguishable clinical outcomes (Table 6). A mild, relatively rapid clinical course was characterized by a transient elevation in temperature with a rapid return to a normal temperature and the early development of a small raised primary lesion, about 2 cm in diameter, at the inoculation site and small discrete secondary lesions on ears, eyelids, and body. Both the primary and secondary lesions rapidly scabbed over. Most rabbits had almost completely recovered from disease by 12 days after infection, with a concomitant return to normal temperatures (Fig. 3). In both groups, one rabbit developed mild



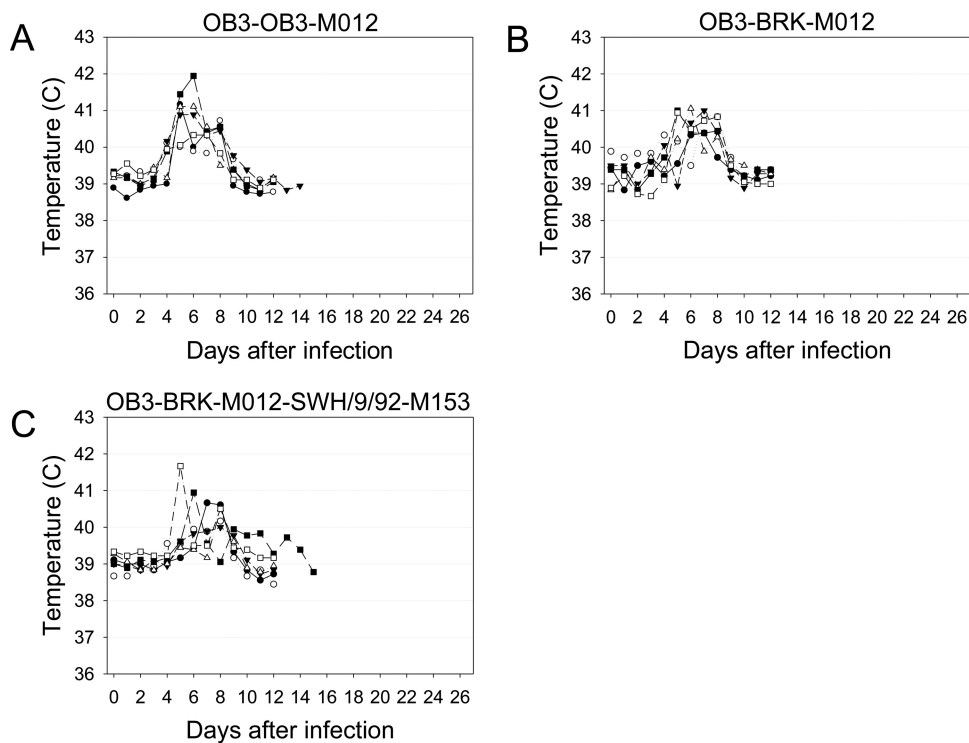


**FIG 3** Daily rectal temperatures of rabbits infected with the reverse-engineered OB3 Y317 viruses. (A) OB3-OB3-M012; (B) OB3-BRK897-M012; (C) OB3-BRK-M012-SWH-M153.

upper respiratory disease with congestion and discharge from the nose and eyes, which delayed recovery.

**OB3 Y317-M012-M153 double-reverse-engineered virus.** We explored the possible role of a single substitution in a known virulence gene by making the double-reverse-engineered virus OB3-BRK-M012-SWH/9/92-M153 with the E177A substitution reversed in M153. The disease course in rabbits infected with this virus was indistinguishable from that seen in rabbits infected with the other OB3 Y317 viruses. (Table 6 and Fig. 3C).

The disease course for all OB3 Y317 infections was much milder and with a shorter duration than those seen with Ur infections.

**Meby-M153 engineered virus.** Meby is a moderately attenuated virus, with the most obvious likely attenuating mutation being a 73-nt deletion in *M153R*. We predicted that the replacement of the Meby *M153R* gene with an intact copy of the gene would significantly enhance the virulence of the virus. Again, this was not the case. Both reverse-engineered Meby viruses were significantly more virulent than Ur; all but 1 of the 12 rabbits were severely affected, and only 2 rabbits infected with the revertant control, Meby-Meby-M153, and 3 rabbits infected with the virus with the intact *M153R* gene, Meby-SWH/9/92-M153, were alive at day 18, when the trial was stopped on humanitarian grounds, as it was clear that the virulence of the reverse-engineered virus had not increased compared to that of the revertant control (Fig. 4A and Table 6). The rabbits developed typical cutaneous myxomatosis: large, raised primary lesions; distinct secondary lesions; and swollen eyelids, ears, head, and anogenital region. The replacement of the Meby *M153R* gene with an intact copy of the gene did not increase the virulence of the reverse-engineered virus compared to that of the revertant control. Indeed, the revertant virus appeared to cause more-severe clinical signs, with four rabbits having an acute syndrome characterized by collapse and pulmonary edema between days 9 and 13. In some of these rabbits, a spike in temperature was seen, followed by a precipitous fall (Fig. 5A and B). The remaining two rabbits were euthanized at day 18 on humanitarian grounds but may have gone on to recover. For the

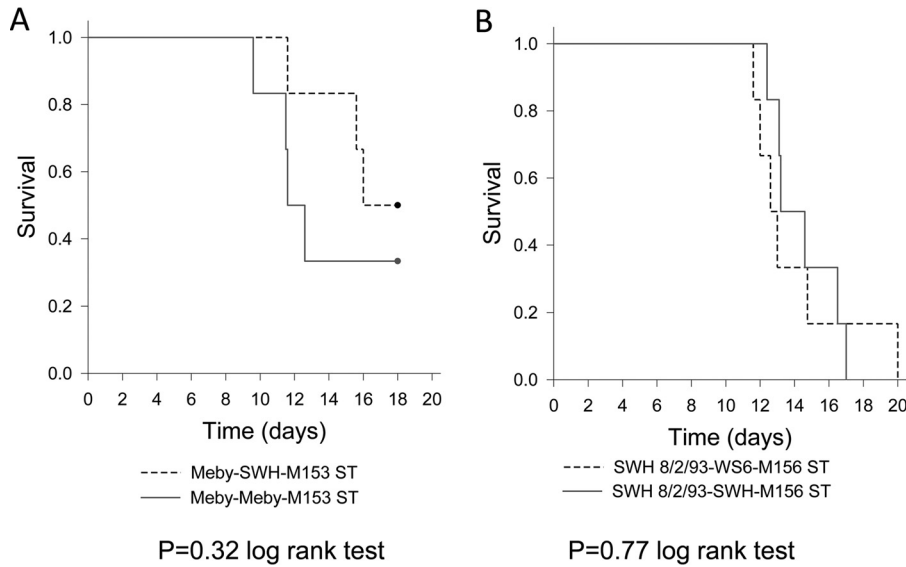


**FIG 4** Kaplan-Meier survival time plots of Meby (A) and SWH 8/2/93 (B) reverse-engineered viruses.

purposes of AST calculations, we arbitrarily treated these rabbits as survivors. For the Meby-SWH/9/2-M153 virus, only two rabbits showed the acute syndrome, at days 12 and 16, while one rabbit had a very mild clinical course and had essentially recovered by day 16. If this rabbit is removed from the ST calculations (Table 6), the AST for the reverse-engineered virus drops to 23 days, although there is still a large difference in ASTs between the revertant virus at 16 days and the reverse-engineered virus. Kaplan-Meier analysis, with the “surviving” rabbits censored, did not show any significant difference between the two viruses (Fig. 4A).

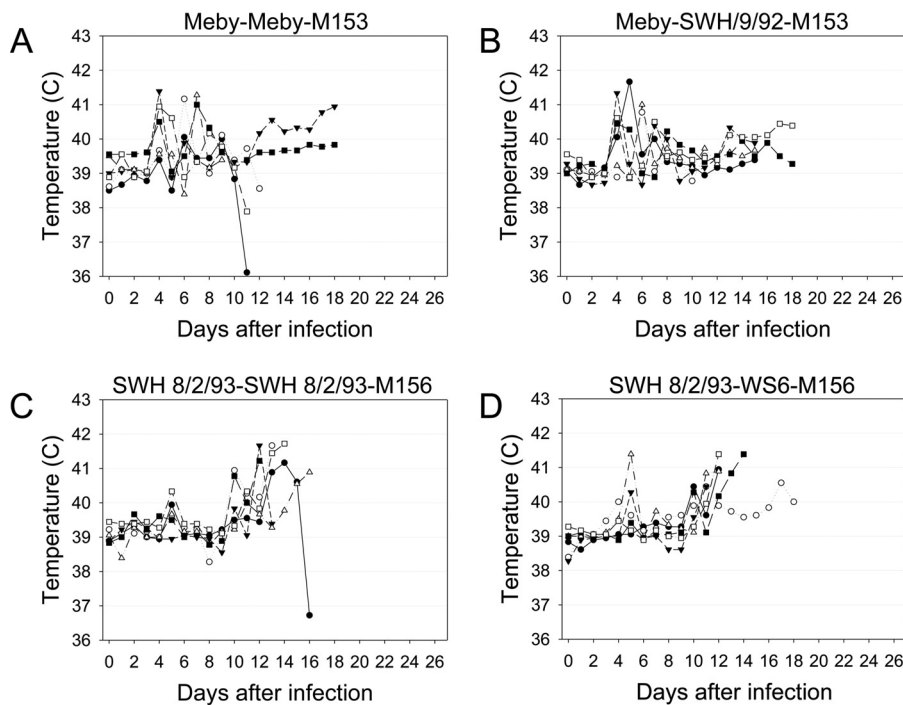


**FIG 5** Daily rectal temperatures of rabbits infected with reverse-engineered Meby and SWH 8/2/93 viruses. (A) Meby-Meby-M153; (B) Meby-SWH/9/92-M153; (C) SWH 8/2/93-SWH 8/2/93-M156; (D) SWH 8/2/93-WS6-M156.

The virulence of the Meby revertant, where four rabbits died acutely and the remaining two may have recovered, fits poorly with the grading system (Table 1) of Fenner and Marshall (18). Based on ASTs, the virus would be classified as a grade 2 or 3A virus, but based on CFRs, it is a grade 3B or 4 virus.

**SWH 8/2/93-M156 reverse-engineered virus.** The L98P substitution in M156 abolishes the inhibition of PKR (33). However, there were no data on whether this caused attenuation in rabbits. We predicted that if this substitution was important for virulence, the insertion of a gene encoding P98 should reduce virulence. Hence, we tested the mutation in a virulent (grade 2) virus background. However, we saw no difference in virulence between the reverse-engineered P98 virus and the revertant L98 virus.

The SWH 8/2/93 viruses were considerably more virulent than the other viruses tested; all rabbits died or were euthanized by day 20 (Fig. 4B and Table 6). Rabbits infected with either the revertant control with L98 or the SWH-WS6-M156 virus with P98 had essentially identical disease that was quite different from the cutaneous nodular myxomatosis seen with Ur or Meby: primary lesions were diffuse, flat, and not clearly demarcated from the surrounding skin, and no secondary cutaneous lesions developed, although most rabbits had swollen ears, eyelids, and heads. This lack of cutaneous lesions is reminiscent of “amyxomatous” myxomatosis, initially described in France in the 1980s (35). However, four rabbits in each group died acutely between days 12 and 15, with a distinct syndrome resembling septic shock with hemorrhage and pulmonary edema (this was similar to the acute deaths in the Meby-infected group). Histologically, there were masses of coccoid bacteria in tissues such as lung, liver, spleen, and lymph nodes but with no apparent cellular inflammatory response. Temperature curves were biphasic, with an initial transient rise at around 5 to 6 days and then a second peak at around 10 to 14 days (Fig. 5C and D). There was no difference in clinical disease or survival times between the SWH 8/2/93-M156 revertant control virus and the SWH-WS6-M156 virus, indicating that the L98P substitution in M156 was not significant for virulence in nonresistant rabbits in the genetic background of this virus.

## DISCUSSION

Moderately attenuated viruses quickly became predominant in the field after the release of MYXV in Australia. By permitting longer survival of rabbits in an infectious state, these viruses had a greater likelihood of transmission than did very virulent viruses (17). We examined the molecular basis of virulence changes during the course of this ongoing host-pathogen coevolution by reverse engineering mutations found in viruses isolated from the field early and late in the evolutionary history. Surprisingly, no single or two mutations tested caused an appreciable change of virulence. This included the replacement of defective copies of *M005L/R* and *M153R* previously defined as being major virulence determinants (31, 32). This suggests that predictions based on single-gene knockout studies with a progenitor virus strain cannot confidently explain the molecular mechanism of virulence changes in field isolates. Indeed, highly virulent MYXV strains with disruptions of reading frames in major virulence genes, including *M005L/R* and *M153R*, have been isolated from the field in Australia and Great Britain (27, 36).

We examined the effects of six mutations in five candidate genes on virulence. None of the mutations could account for the pronounced differences in virulence detected during the radiation of MYXV after the highly virulent SLS was released in 1950. We now discuss each gene in turn.

***M005L/R*.** Ur was the first well-characterized highly attenuated field isolate made following the spread of MYXV in Australia (30, 37). Ur has minimal genetic divergence from the SLS progenitor, with only 8 nucleotide substitutions and 5 single-nucleotide indels (2 of which are intergenic). The disruption in *M005L/R*, a well-characterized virulence gene, suggested a ready explanation for attenuation, and we predicted that it would be straightforward to demonstrate a stepwise increase in virulence when the

mutant *M005L/R* gene in Ur was replaced by the *M005L/R* genes from SLS and Lu. Strikingly, however, no change in phenotype was observed in laboratory rabbits or during replication in the CD4<sup>+</sup> T lymphocyte cell line RL-5. Our results are therefore in contrast with the dramatically attenuated phenotype shown by the Lu *M005L/R* gene knockout (31) and led us to question the role of *M005L/R* in SLS and subsequent Australian viruses.

The frameshift mutations in *M005L/R* found in Australian isolates are noteworthy because M005 has been defined as a major virulence factor with multiple functions and is necessary for productive infection in lymphocytes, which is regarded as being critical for virus dissemination in infected rabbits (31, 38, 39). The deletion of *M005L/R* from Lu attenuated the virus, with the CFR falling from 100% to 0 (31). In the progenitor SLS virus released in 1950, there is a C insert after nucleotide 34 of *M005L/R*; all of the Australian isolates sequenced to date have this mutation (27, 28). This indel disrupts the predicted ORF of *M005L/R*. However, based on prerelease testing and early-epidemic estimates, the CFR for SLS was as high as 99.8% (40–44). In addition, SLS can still replicate in lymphocytes of resistant wild rabbits and susceptible laboratory rabbits (45), and in laboratory rabbits, its virulence was similar to that of Lu (18). To explain the high virulence of SLS, it was speculated that an alternative ATG codon at positions 17 to 19 could be used as a start codon (27). This would correct the reading frame to express M005 with a minor sequence alteration at the N terminus compared to the Lu reference sequence. Inefficient use of the alternate ATG codon could potentially explain the lower virulence of SLS than of Lu when the viruses were tested in genetically resistant rabbits (44). A second C insertion at the same position (after nucleotide 34) in *M005L/R* in Ur means that the alternative ATG codon cannot correct the ORF in this attenuated virus.

SLS is probably derived from a virus isolated in Brazil in around 1910 (46) and was maintained by serial passage in laboratory rabbits over many years prior to 1950. Hence, SLS may have adapted to European rabbits before its spread in Australia, possibly including epistatic mutations that compensated for a defective *M005L/R* gene. Recent virulent MYXV isolates from Britain, and, thus, derived from Lu, have lost the active site of M005 in the C terminus of the protein, again suggesting that the loss of this gene can be compensated for by other mutations (36).

**M014L.** The frameshift mutation in Ur *M014L* leads to a loss of the most C-terminal Kelch domain, which is presumed to be important for substrate interactions (47). This mutation was observed in two other early strains: Glenfield, a strain with higher virulence than SLS (when tested in resistant rabbits) isolated in early 1951, and KM13, a moderately attenuated strain isolated in 1952 (18, 27, 48). Since Glenfield was isolated only 2 months after the initial spread of SLS, this mutation must have occurred early in the Australian MYXV radiation but has been subsequently lost in the virus populations that we have sampled. The finding that the same mutation is present in MYXV strains with high, medium, and low virulence suggests that this mutation alone is not a good predictor of phenotype. Consistent with this observation, the replacement of the disrupted Ur *M014L* gene with the intact SLS *M014L* gene did not increase the virulence of Ur.

**M012.** OB3 Y317 is the most attenuated field isolate documented to date in Australia. M012 is a dUTPase that catalyzes the dephosphorylation of dUTP to dUMP to minimize its incorporation into genomic DNA. The 13-nt deletion in *M012L* in OB3 Y317 truncates the M012 protein after 70 amino acids (aa) (normally 148 aa) and would be predicted to disrupt assembly into the active homotrimer, as well as deleting residues contributing to the active site (49). However, the restoration of an intact *M012L* gene did not increase the virulence of OB3 Y317. The vaccinia virus (VACV) orthologue of M012, F2L, is not an important virulence factor (50, 51), and the protein is potentially at least partially redundant due to the uracil-DNA glycosylase activity encoded by *M079R*. Interestingly, in Epstein-Barr virus infection, the viral dUTPase is a pathogen-associated molecular pattern molecule that activated NF- $\kappa$ B signaling through Toll-like

receptor 2 (TLR-2) (52). This suggests that the attenuation of OB3 Y317 is likely due to one or more point mutations rather than to gene disruption. However, we can exclude a role for the E177A substitution in M153.

**M153.** We reverse engineered two mutations in M153 in different parental backgrounds, and neither mutation restored virulence. M153 is an E3 ubiquitin ligase with a RING finger-like domain and 2 transmembrane domains plus a C-terminal conserved region (CR). It downregulates the cell surface expression of major histocompatibility complex class I (MHC-I), ALCAM-1, CD95, and CD4 (32, 53, 54). The deletion of *M153R* in the Lu-derived T1 strain severely attenuated the virus, with a case fatality rate of 30%, compared with a case fatality rate of 100% for the parental virus (32). In Meby, there is a deletion of 73 nt in *M153R*, which replaces the highly acidic C-terminal domain critical for MHC-I downregulation (55) with an unrelated and arginine-rich sequence. However, the replacement of the Meby *M153R* gene with an intact copy of *M153R* did not cause any increase in virulence (Table 6 and Fig. 4A). Interestingly, the virulent Glenfield strain also has a disrupted *M153R* ORF, and the reading frame is also disrupted in some other modern Australian isolates (27, 28). In some field isolates of MYXV from Great Britain, the disruption of *M153R* is compatible with high virulence (36).

**M156.** The M156 L98P substitution was of interest because it has occurred independently on two branches of the phylogenetic tree of Australian MYXV, has been demonstrated to abrogate PKR inhibition, and has been proposed as a major modulator of virulence during MYXV evolution in Australia (28, 33). M156 has sequence similarity to the mammalian  $\alpha$  subunit of eukaryotic initiation factor 2 (eIF2 $\alpha$ ) as well as to a family of viral proteins that bind to interferon-induced PKR and inhibit the phosphorylation of eIF2 $\alpha$  (56). This mutation abolished PKR inhibition (33). However, the replacement of the L98 *M156R* gene with the P98 *M156R* gene did not cause any reduction in virulence in the grade 2 virulent SWH 8/2/93 strain. It is possible that this mutation is meaningful only in resistant wild rabbits. However, based on the lack of an effect in the SWH 8/2/93 genetic background, it seems likely that if this mutation has played a role in the attenuation of MYXV, it is compensated for in this genetic background. It is interesting that the MYXV *M029L* gene encodes a multifunctional protein that inhibits PKR and is essential for replication in RL-5 cell culture (34), whereas *M156R* was not essential in RL-5 cell culture. It is possible that *M156R* is redundant in European rabbits, although this gene has been duplicated in a lineage of Australian viruses (28). Other workers have demonstrated that the VACV orthologue K3L is able to rapidly adapt to mutations in PKR in an artificial-selection system, suggesting that this protein is important in poxvirus evolution (57).

**Conclusion.** In summary, it is striking that none of the mutations reverse engineered in this study showed an appreciable impact on virulence. There are several possible explanations for this. First, it is possible that we simply failed to test the mutations responsible for alterations in virulence. Indeed, resource constraints and technical limitations meant that we could not test all genetic differences that could account for the phenotypic differences between the virulent SLS progenitor and its attenuated descendants. Even in the highly attenuated Ur virus, which has only limited genetic differences from SLS, there are three disrupted ORFs, and we were able to test only two. It is formally possible the loss of the C terminus of M134 could be responsible for attenuation. However, a definitive statement cannot be made until this disruption is directly tested. This protein is orthologous to B22R in *Variola virus* and is present in the virions of *Cowpox virus* and *Monkeypox virus* (MPXV), although it was not reported in a proteomic study of MYXV virions (58–60). This protein is conserved in chordopoxviruses, but it is not expressed in VACV (59, 61), and its length is highly variable, even among the leporipoxviruses. Orthopoxvirus B22R orthologues have a T cell suppressor function, and a deletion mutant of MPXV was attenuated in a nonhuman primate model (62). A second possibility is that combinations of mutations interacting epistatically played a critical role in the ongoing evolution of MYXV virulence after it jumped into its new host, and, with two exceptions, we did not test for polygenic effects. A third



possibility is that genetic differences in noncoding regions are involved, and none of these changes were tested in this study.

Our previous work showed that the relatively large MYXV genome, combined with multiple, possibly redundant, mechanisms for suppressing host immune responses to infection, has allowed the virus to explore many pathways that lead to success in the field. In wild rabbits in Australia, this is occurring in the face of very strong selection for genetic resistance to myxomatosis (21, 22, 45, 63). The search for the genetic basis of MYXV virulence evolution is hampered by the absence of convergence at the genetic level. Hence, the genetic basis for any example of attenuation in the field in this canonical case of virulence evolution remains mysterious.

## MATERIALS AND METHODS

**Viruses and cells.** MYXV strains Lausanne (Lu) (Brazil/Campinas/1949) (GenBank accession number [NC\\_001132](#)), SLS (Brazil/1910) (accession number [JX565574](#)), Australia/Uriarra/1953 (Ur) (accession number [JX565577](#)), Australia/SWH/8-2-93/1993 (SWH 8/2/93) (accession number [JX565575](#)), Australia/OB3/Y317/1994 (OB3 Y317) (accession number [KC660083](#)), Australia/Meby/1991 (Meby) (accession number [JX565571](#)), Australia/BRK 897/1995 (BRK 897) (accession number [JX565564](#)), Australia/WS61071/1995 (WS6/1071) (accession number [JX565580](#)), and Australia/SWH/9-1992 (SWH 9/92) (accession number [JX565576](#)) were used in this study. The rabbit kidney cell line RK13 was propagated in Eagle's minimum essential medium (EMEM), and the rabbit CD4<sup>+</sup> T lymphocyte cell line RL-5 was cultured in RPMI 1640 medium, both with 10% fetal calf serum (FCS), 100 U penicillin/ml, and 100  $\mu$ g streptomycin/ml (Sigma-Aldrich), at 37°C with 5% CO<sub>2</sub>.

**Construction of knockout and knock-in plasmids for reverse genetics.** Genes in MYXV are numbered according to the system described previously by Cameron et al. (25), with the gene in italic type and the direction of transcription being shown as left (L) or right (R); genes in the TIR are shown as L/R, e.g., *M005L/R*. Proteins are identified by the gene number but with the direction of transcription omitted and without italic type, e.g., M005. It has now been demonstrated that the *M156R* gene is transcribed from an early promoter and an ATG sequence at codon 28 in the annotated sequence (33, 64), leading to a predicted protein of 75 aa rather than 102 aa. For simplicity, we have retained the annotated numbering here.

A two-step process was used for reverse engineering. The target gene was initially replaced with the mCherry red fluorescence gene as a selectable marker, while in the second step, the mCherry gene was replaced with the replacement MYXV gene or the original MYXV gene as a control. A shuttle vector for knocking out each target gene in the parental virus was constructed by using the pGEM-T plasmid (Promega). A red fluorescence mCherry protein expression cassette driven by a poxvirus early/late promoter, pSS (65, 66), was inserted into the multiple-cloning sites of pGEM-T with additional restriction enzyme sites to facilitate the insertion of the flanking sequence from both sides of the target genes to enable homologous recombination with the viral genome. The genes amplified and the flanking sequences are shown in Fig. S1 in the supplemental material.

Total DNA was extracted from virus-infected RK13 cells by using the DNeasy blood and tissue kit (Qiagen). Target fragments were amplified by PCR using the primers listed in Table 7. To construct plasmids for knocking out target genes, approximately 300 bp of flanking sequences on the left and right sides of the target genes (named FS1 and FS2, respectively, for brevity) were amplified by PCR using the respective primers. In practice, the constraints of the surrounding sequence meant that flanking sequences varied from 252 to 330 bp and in some cases included the 5' or 3' end of the gene of interest. Purified fragments were inserted at the left and right sides of the mCherry gene. The knockout plasmids were named pGEM-FS1-mCherry-FS2 according to each target gene.

To construct plasmids for knocking in target genes, each gene, including FS1 and FS2, was amplified as one fragment by PCR. The purified fragments were cloned into a pGEM-T plasmid, named according to each target gene. Nucleotide sequences were confirmed by Sanger sequencing for all the cloned genes.

**Production of knockout viruses.** To knock out the target gene in the parental virus, RK13 cells were infected with the parental virus at a multiplicity of infection (MOI) of 3 for 1 h. Next, 0.5  $\mu$ g of the knockout plasmid pGEM-FS1-mCherry-FS2 was transfected into the cells by using Lipofectamine 3000 reagent, according to the manufacturer's protocol (Invitrogen). After 2 days, cells and medium were freeze-thawed three times and centrifuged to clarify the virus, and virus in the supernatant was retained for a virus stock. In the first round of plaque purification, the virus stock was diluted 1:1,000 to 1:4,000 before infection of RK13 cells seeded into 96-well plates. After 5 to 7 days, 24 individual virus plaques with red fluorescence were picked, and each plaque was resuspended in 100  $\mu$ l of medium; this suspension was further diluted 1:400 and used to infect RK13 cells in a 96-well plate. After 4 to 5 cycles of plaque-to-plaque purification, 60  $\mu$ l of virus from individual plaque-purified stocks was used to infect RK13 cells in duplicate wells (30  $\mu$ l/each) of a 12-well plate. After 4 days, all virus plaques were examined by fluorescence microscopy. Cells were harvested only when all the virus plaques in both wells showed red fluorescence and no nonfluorescing plaques were present.

Cells in one well were washed with cold phosphate-buffered saline (PBS) (pH 7.4) twice and harvested in 200  $\mu$ l of PBS for extraction of total DNA by using the DNeasy blood and tissue kit (Qiagen). Total DNA was used as the template for PCR. The difference in size between FS1-mCherry-FS2 and FS1-target-gene-



**TABLE 7** Target genes and primers used for cloning in this study<sup>a</sup>

Target gene	Primer	Purpose of primer	Sequence (position-5'-3' sequence-position)
<i>mCherry</i>	MP1	Forward primer for <i>mCherry</i>	<u>CTCGAGGGATCCTCTAGAAAGCTT</u> CACACCGCATACAGGTGGCAC
	MP2	Reverse primer for <i>mCherry</i>	GAATTCGGTACCAGATCTCCCGGGT <u>AGCCCTCCACACATAAC</u>
<i>M005L/R</i>	MP3	Forward primer for FS1	155083- <u>CCGCTCGAGCGGGTCGGAGGACGTACGAAAC</u> -155100 <sup>b</sup>
	MP4	Reverse primer for FS1	155363-GCTCTAGAGCCCTCGTCCGGGGTTATATC-155381
	MP5	Forward primer for FS2	156861-GAAGATCTTCCCTATTTGGTAGGCTCTATCC-156881
	MP6	Reverse primer for FS2	157153-GGAATTCATATGGAAATCCCATGTTCTACCTC-157169
<i>M012L</i>	MP7	Forward primer for FS1	13800-CGGGATCCCGTACTTCCGAGAACATAGCCGCGTC-13824
	MP8	Reverse primer for FS1	14104-CCCAAGCTTGGGCGTCGATGATGTCTCGTTTAAAGACG-14129
	MP9	Forward primer for FS2	14620-GAAGATCTTCGACATACACCTCGTTGCTTCTTCGG-14644
	MP10	Reverse primer for FS2	14883-CGGAATTCGCGATGGAGGACCTATACATCGAACG-14907
<i>M014L</i>	MP11	Forward primer for FS1	14847-CGGGATCCCGGCCAGGTCTATTCTGTGCGATC-14867
	MP12	Reverse primer for FS1	15109-CCCAAGCTTGGGGAGTCTTGTCTGTTCTGGGAG-15130
	MP13	Forward primer for FS2	16676-GAAGATCTTCGGTAATCGCTAACGCGTTTTTCG-16698
	MP14	Reverse primer for FS2	16919-CGGAATTCGCGATACACCGTCCGAGGAACGAG-16940
<i>M153R</i>	MP15	Forward primer for FS1	148269-CGGGATCCCGCGGAAACGGGACACAACGTAACG-148291
	MP16	Reverse primer for FS1	148505-CCCAAGCTTGGGCGTAGCCATGTTTACACAAC-148526
	MP17	Forward primer for FS2	149238-GAAGATCTTCGGTATCTCGTTTGTCTATAACAAAGATCG-149266
	MP18	Reverse primer for FS2	149479-CGGAATTCGCGGCAATCAACTCCCGACTCG-149500
<i>M156R</i>	MP19	Forward primer for FS1	149948-CGGGATCCCGTAACAACACGTGTGCTGAGCG-149970
	MP20	Reverse primer for FS1	150178-CCCAAGCTTGGGGTGTCTTGCCTGTAGTTCAGAT-150199
	MP21	Forward primer for FS2	150358-GAAGATCTTCGGACTATGGACGTTCCGATACGTC-150381
	MP22	Reverse primer for FS2	150597-CGGAATTCGCGACGCGTTGCACGGAGGTATTG-150618

<sup>a</sup>Restriction sites in primers are underlined; the 2 or 3 bases on either side of the restriction site were added as spacers.

<sup>b</sup>Sequence positions are for the SLS genome (GenBank accession number [JX565574](#)).

FS2 following agarose gel electrophoresis was used to confirm the production of the knockout virus and to exclude the presence of the original genes. Cells in the second well were used to prepare a virus stock.

**Single-gene knock-in viruses.** To insert the replacement genes into the knockout virus, RK13 cells in 24-well plates were infected with the knockout virus at an MOI of 3 for 1 h, and the knock-in plasmid pGEM-FS1-target-gene-FS2 was then transfected into cells. After 4 to 5 rounds of plaque-to-plaque purification for the knock-in virus with no red fluorescence, PCR was performed by using the total DNA extracted from RK13 cells infected with the knock-in virus. The PCR products were checked by agarose gel electrophoresis to confirm the presence of the target gene and the absence of the *mCherry* gene. The PCR fragment was gel purified and cloned into a pGEM-T plasmid. At least three clones for each virus were sequenced. Only the virus for which all three clones had the correct sequence was used to prepare the knock-in virus stocks.

**Double-gene knock-in viruses.** The mutation in the Ur *M014L* gene of the reverse-engineered Ur-SLS-M014 virus was repaired by using *M014L* from SLS, and this virus was used as a parental virus to produce the Ur-SLS-M014-Lu-M005 virus, in which the Ur *M005L/R* gene was replaced by *M005L/R* from Lu. Plasmid pGEM-FS1-*mCherry*-FS2-M005 was used to knock out Ur *M005L/R*, and plasmid pGEM-FS1-M005-FS2 (Lu) was used to knock in Lu *M005L/R*.

*M012L* in OB3 Y317 was replaced by an intact *M012L* gene from BRK 897, and the resulting OB3-BRK-M012 virus was used as the parental virus to produce the OB3-BRK-M012-SWH9-M153 virus, in which OB3 Y317 *M153R* was replaced by *M153R* from SWH 9/92. Plasmid pGEM-FS1-*mCherry*-FS2-M153 was used to knock out *M153R*, and plasmid pGEM-FS1-M153-FS2 (SWH) was used to knock in *M153R*. Control revertant viruses were not made for the double-reverse-engineered viruses, but the entire genome was sequenced to confirm that no secondary mutations had occurred (see below).

**Genomic sequencing of reverse-engineered viruses.** We confirmed the sequences of each target gene in the knock-in viruses by Sanger sequencing and also checked whether other mutations were introduced during the process of plaque purification by sequencing the whole genomes of all 13 reverse-engineered viruses. Viral DNA was extracted from infected cells and sequenced by using Nextera XT prepared libraries on an Illumina MiSeq instrument (v2 500 cycle kit), with final genome assembly being performed as described previously (36, 67).

**Virus replication analysis.** For multistep growth analysis,  $2 \times 10^5$  RL-5 cells were infected at an MOI of 0.05 in 200  $\mu$ l of RPMI-10% FCS. After 1 h of virus adsorption at 37°C, cells were washed once with RPMI-10% FCS, resuspended in 1 ml of RPMI-10% FCS, and seeded into 24-well plates in triplicate. The time point of seeding of virus-infected cells was assigned as 0 h. Cells in 1 ml of medium were harvested at 4, 8, 20, 28, 44, 52, and 68 h postinfection (hpi), and viruses were released by three freeze-thaw-vortexing cycles and then centrifuged at 5,000 rpm for 1 min. The 1-ml supernatant was assayed on RK13 cells in 12-well plates, and the virus titer was expressed as PFU per milliliter. Single-step growth analysis was performed with RL-5 cells at an MOI of 5; cells were harvested at 4, 8, 20, 28, and 44 hpi; and titers were determined as described above.

**Ethics statement.** Animal studies were carried out at The Pennsylvania State University (University Park, PA, USA) in accordance with recommendations in the *Guide for the Care and Use of Laboratory Animals* (68). The protocol used for animal experiments was approved by the Animal Care and Use Committee of The Pennsylvania State University (approval number 42748).

**Rabbit experiments.** Outbred 4-month-old male New Zealand White rabbits (*Oryctolagus cuniculus*) were purchased from Harlan Laboratory. Rabbits were specific pathogen free (SPF) for *Bordetella bronchiseptica*, *Pasteurella multocida*, as well as a range of other pathogens and parasites. For the trials with the two double-reverse-engineered viruses, rabbits were purchased from Charles River Laboratories and were similarly SPF for *B. bronchiseptica* and *P. multocida*. Rabbits were maintained on 125 g of standard rabbit pellets per day with *ad lib* water in individual cages and allowed to acclimate for 10 days in the facility prior to the start of experiments.

Six rabbits were used to test each virus construct. For each rabbit, 100 PFU of virus resuspended in 100  $\mu$ l of Dulbecco's modified Eagle medium (DMEM) was inoculated intradermally in the right rump. Rabbits were examined twice daily: rectal temperature was determined; body weight was measured; the size of primary lesion was measured; the number and distribution of secondary lesions were estimated; a semiquantitative score of 0 to 3 was given for the degrees of eyelid swelling, blepharconjunctivitis, ear swelling, nasal discharge, respiratory difficulty, anogenital swelling, scrotal swelling, and demeanor; food intake and water intake were recorded; and fecal and urine outputs were monitored by inspection of the waste trays. Rabbits were euthanized based on the degree of clinical severity, using respiratory difficulty, depression, inanition, reluctance to move, weakness upon handling, weight loss, and failure to eat or drink as indicators. Any rabbit exhibiting pain or with a subnormal temperature was immediately euthanized. Where possible, trials were terminated once it became obvious that there was no difference between virus phenotypes.

To allow comparison with data from previous work, STs in days were normalized as  $\log_{10}(\text{ST} - 8)$ , used to calculate ASTs, and then back-transformed; rabbits that were alive at the end of the trial were assigned an ST of 60 days (18). Virulence grades were assigned as described previously by Fenner and Marshall (18) and Fenner and Woodroffe (19) (Table 1). Kaplan-Meier survival plots were based on actual survival times and tested for differences by using a log rank test implemented in SigmaPlot.

## SUPPLEMENTAL MATERIAL

Supplemental material for this article may be found at <https://doi.org/10.1128/JVI.01289-17>.

**SUPPLEMENTAL FILE 1**, PDF file, 0.4 MB.

## ACKNOWLEDGMENTS

This work was funded by grant R01 AI093804 from the National Institute of Allergy and Infectious Diseases, National Institutes of Health. E.C.H. was funded by a National Health and Medical Research Council Australia fellowship (GNT1037231). J.-S.E. is supported by an NHMRC early-career fellowship (1073466). Part of the work done by J.L. was supported by the Winston Churchill Memorial Trust.

We thank Karen Glover and Andrew Walker for technical support and David Tschärke for providing plasmids with the mCherry and promoter constructs.

## REFERENCES

- Pepin KM, Lass S, Pulliam JRC, Read AF, Lloyd-Smith JO. 2010. Identifying genetic markers of adaptation for surveillance of viral host jumps. *Nat Rev Microbiol* 8:802–813. <https://doi.org/10.1038/nrmicro2440>.
- Yip CW, Hon CC, Shi M, Lam TT-L, Chow KY-C, Zeng F, Leung FC-C. 2009. Phylogenetic perspectives on the epidemiology and origins of SARS and SARS-like coronaviruses. *Infect Gen Evol* 9:1185–1196. <https://doi.org/10.1016/j.meegid.2009.09.015>.
- Brault AC, Huang CY, Langevin SA, Kinney RM, Bowen RA, Ramey WN, Panella NA, Holmes EC, Powers AM, Miller BR. 2007. A single positively selected West Nile viral mutation confers increased virulence in American crows. *Nat Genet* 39:1162–1166. <https://doi.org/10.1038/ng2097>.
- Tsetsarkin KA, Vanlandingham DL, McGee CE, Higgs S. 2007. A single mutation in chikungunya virus affects vector specificity and epidemic potential. *PLoS Pathog* 3:e201. <https://doi.org/10.1371/journal.ppat.0030201>.
- Anderson RM, May RM. 1982. Coevolution of hosts and parasites. *Parasitology* 85:411–426. <https://doi.org/10.1017/S0031182000055360>.
- Bull JJ. 1994. Virulence. *Evolution* 48:1423–1437. <https://doi.org/10.1111/j.1558-5646.1994.tb02185.x>.
- Pfennig KS. 2001. Evolution of pathogen virulence: the role of variation in host phenotype. *Proc Biol Sci* 268:755–760. <https://doi.org/10.1098/rspb.2000.1582>.
- MacKinnon MJ, Read AF. 2004. Immunity promotes virulence evolution in a malaria model. *PLoS Biol* 2:e230. <https://doi.org/10.1371/journal.pbio.0020230>.
- Mackinnon MJ, Read AF. 2004. Virulence in malaria: an evolutionary viewpoint. *Philos Trans R Soc Lond B Biol Sci* 359:965–986. <https://doi.org/10.1098/rstb.2003.1414>.
- Ebert D, Bull JJ. 2003. Challenging the trade-off model for the evolution of virulence: is virulence management feasible? *Trends Microbiol* 11:15–20. [https://doi.org/10.1016/S0966-842X\(02\)00003-3](https://doi.org/10.1016/S0966-842X(02)00003-3).
- Bull JJ, Luring AS. 2014. Theory and empiricism in virulence evolution. *PLoS Pathog* 10:e1004387. <https://doi.org/10.1371/journal.ppat.1004387>.
- Read AF, Baigent SJ, Powers C, Kgosana LB, Blackwell L, Smith LP, Kennedy DA, Walkden-Brown SW, Nair VK. 2015. Imperfect vaccination can enhance the transmission of highly virulent pathogens. *PLoS Biol* 13:e1002198. <https://doi.org/10.1371/journal.pbio.1002198>.
- Fenner F, Fantini B. 1999. Biological control of vertebrate pests: the history of myxomatosis, an experiment in evolution. CAB International, New York, NY.
- Fenner F. 1983. Biological control as exemplified by smallpox eradication and myxomatosis. *Proc R Soc Lond B Biol Sci* 218:259–285. <https://doi.org/10.1098/rspb.1983.0039>.

15. Dwyer G, Levin S, Buttel L. 1990. A simulation model of the population dynamics and evolution of myxomatosis. *Ecol Monogr* 60:423–447. <https://doi.org/10.2307/1943014>.
16. Kerr PJ. 2012. Myxomatosis in Australia and Europe: a model for emerging infectious diseases. *Antiviral Res* 93:387–415. <https://doi.org/10.1016/j.antiviral.2012.01.009>.
17. Fenner F, Day MF, Woodroffe GM. 1956. Epidemiological consequences of the mechanical transmission of myxomatosis by mosquitoes. *J Hyg (Lond)* 54:284–303. <https://doi.org/10.1017/S0022172400044521>.
18. Fenner F, Marshall ID. 1957. A comparison of the virulence for European rabbits (*Oryctolagus cuniculus*) of strains of myxoma virus recovered in the field in Australia, Europe and America. *J Hyg (Lond)* 55:149–191. <https://doi.org/10.1017/S0022172400037098>.
19. Fenner F, Woodroffe GM. 1965. Changes in the virulence and antigenic structure of strains of myxoma virus recovered from Australian wild rabbits between 1950 and 1964. *Aust J Exp Biol Med Sci* 43:359–370. <https://doi.org/10.1038/icb.1965.69>.
20. Fenner F, Ross J. 1994. Myxomatosis, p 205–240. *In* Thompson HV, King CM (ed), *The European rabbit: the history and biology of a successful colonizer*. Oxford University Press, Oxford, England.
21. Marshall ID, Fenner F. 1958. Studies in the epidemiology of infectious myxomatosis of rabbits. V. Changes in the innate resistance of wild rabbits exposed to myxomatosis. *J Hyg (Lond)* 56:288–302. <https://doi.org/10.1017/S0022172400037773>.
22. Marshall ID, Douglas GW. 1961. Studies in the epidemiology of infectious myxomatosis of rabbits. VIII. Further observations on changes in the innate resistance of Australian wild rabbits exposed to myxomatosis. *J Hyg (Lond)* 59:117–122. <https://doi.org/10.1017/S0022172400038766>.
23. Ross J, Sanders MF. 1984. The development of genetic resistance to myxomatosis in wild rabbits in Britain. *J Hyg (Lond)* 92:255–261. <https://doi.org/10.1017/S0022172400064494>.
24. Ross J, Sanders MF. 1987. Changes in the virulence of myxoma virus strains in Britain. *Epidemiol Infect* 98:113–117. <https://doi.org/10.1017/S0950268800061781>.
25. Cameron C, Hota-Mitchell S, Chen L, Barrett J, Cao J-X, Macaulay C, Willer D, Evans D, McFadden G. 1999. The complete DNA sequence of myxoma virus. *Virology* 264:298–318. <https://doi.org/10.1006/viro.1999.0001>.
26. Morales M, Ramirez MA, Cano MJ, Parraga M, Castilla J, Perez-Ordoyo LI, Torres JM, Barcena J. 2009. Genome comparison of a nonpathogenic myxoma virus field strain with its ancestor, the virulent Lausanne strain. *J Virol* 83:2397–2403. <https://doi.org/10.1128/JVI.02189-08>.
27. Kerr PJ, Ghedin E, DePasse JV, Fitch A, Cattadori IM, Hudson PJ, Tschärke DC, Read AF, Holmes EC. 2012. Evolutionary history and attenuation of myxoma virus on two continents. *PLoS Pathog* 8:e1002950. <https://doi.org/10.1371/journal.ppat.1002950>.
28. Kerr PJ, Rogers MB, Fitch A, DePasse JV, Cattadori IM, Twaddle AC, Hudson PJ, Tschärke DC, Read AF, Holmes EC, Ghedin E. 2013. Genome scale evolution of myxoma virus reveals host pathogen adaptation and rapid geographic spread. *J Virol* 87:12900–12915. <https://doi.org/10.1128/JVI.02060-13>.
29. Kerr PJ, Liu J, Cattadori IM, Ghedin E, Read AF, Holmes EC. 2015. Myxoma virus and the leporipoxviruses: an evolutionary paradigm. *Viruses* 7:1020–1061. <https://doi.org/10.3390/v7031020>.
30. Mykytowycz R. 1953. An attenuated strain of the myxomatosis virus recovered from the field. *Nature* 172:448–449. <https://doi.org/10.1038/172448a0>.
31. Mossman K, Lee SF, Barry M, Boshkov L, McFadden G. 1996. Disruption of M-T5, a novel myxoma virus gene member of the poxvirus host range superfamily, results in dramatic attenuation of myxomatosis in infected European rabbits. *J Virol* 70:4394–4410.
32. Guérin JL, Gelfi J, Boullier S, Delverrier M, Bellanger FA, Bertagnoli S, Drexler I, Sutter G, Messud-Petit F. 2002. Myxoma virus leukemia-associated protein is responsible for major histocompatibility complex class I and Fas-CD95 down-regulation and defines scrapins, a new group of surface cellular receptor abductor proteins. *J Virol* 76:2912–2923. <https://doi.org/10.1128/JVI.76.6.2912-2923.2002>.
33. Peng C, Haller SL, Rahman MM, McFadden G, Rothenburg S. 2016. Myxoma virus M156 is a specific inhibitor of rabbit PKR but contains a loss-of-function mutation in Australian virus isolates. *Proc Natl Acad Sci U S A* 113:3855–3860. <https://doi.org/10.1073/pnas.1515611113>.
34. Rahman MM, Liu J, Chan WM, Rothenburg S, McFadden G. 2013. Myxoma virus protein M029 is a dual function immunomodulator that inhibits PKR and also conscripts RHA/DHX9 to promote expanded host-tropism and viral replication. *PLoS Pathog* 9:e1003465. <https://doi.org/10.1371/journal.ppat.1003465>.
35. Joubert L, Ducloux P, Toailen P. 1982. La myxomatose des garennes dans le sud-est. La myxomatose amyxomatose. *Rev Med Vet* 133:739–753.
36. Kerr PJ, Cattadori IM, Rogers MB, Fitch A, Geber A, Liu J, Sim DG, Boag B, Eden J-S, Ghedin E, Read AF, Holmes EC. 2017. Genomic and phenotypic characterization of myxoma virus from Great Britain reveals multiple evolutionary pathways distinct from those in Australia. *PLoS Pathog* 13:e1006252. <https://doi.org/10.1371/journal.ppat.1006252>.
37. Mykytowycz R. 1956. The effect of season and mode of transmission on the severity of myxomatosis due to an attenuated strain of the virus. *Aust J Exp Biol Med Sci* 34:121–132. <https://doi.org/10.1038/icb.1956.15>.
38. Johnston JB, Wang G, Barrett JW, Nazarian SH, Colwill K, Moran M, McFadden G. 2005. Myxoma virus M-T5 protects infected cells from the stress of cell cycle arrest through its interaction with host cell cullin-1. *J Virol* 79:10750–10763. <https://doi.org/10.1128/JVI.79.16.10750-10763.2005>.
39. Werden SJ, Barrett JW, Wang G, Stanford MM, McFadden G. 2007. M-T5, the ankyrin repeat, host range protein of myxoma virus, activates Akt and can be functionally replaced by cellular PIKE-A. *J Virol* 81:2340–2348. <https://doi.org/10.1128/JVI.01310-06>.
40. Martin CJ. 1936. Observations on myxomatosis cuniculi (Sanarelli) made with a view to the use of the virus in the control of rabbit plagues. CSIR Australia research bulletin, no 96. CSIR, Melbourne, Australia.
41. Bull LB, Dickinson CG. 1937. The specificity of the virus of rabbit myxomatosis. *J CSIR* 10:291–294.
42. Bull LB, Mules MW. 1944. An investigation of *myxomatosis cuniculi* with special reference to the possible use of the disease to control rabbit populations in Australia. *J CSIR* 17:79–93.
43. Myers K. 1954. Studies in the epidemiology of infectious myxomatosis of rabbits. II. Field experiments, August–November 1950, and the first epizootic of myxomatosis in the riverine plain of south-eastern Australia. *J Hyg (Lond)* 52:47–59. <https://doi.org/10.1017/S0022172400027248>.
44. Fenner F, Ratcliffe FN. 1965. *Myxomatosis*. Cambridge University Press, Cambridge, England.
45. Best SM, Kerr PJ. 2000. Coevolution of host and virus: the pathogenesis of virulent and attenuated strains of myxoma virus in resistant and susceptible European rabbits. *Virology* 267:36–48. <https://doi.org/10.1006/viro.1999.0104>.
46. Moses A. 1911. O virus do mixoma dos coelhos. *Mem Inst Oswaldo Cruz* 3:46–53. <https://doi.org/10.1590/S0074-02761911000100003>.
47. Zhang L, Villa NY, McFadden G. 2009. Interplay between poxviruses and the cellular ubiquitin/ubiquitin-like pathways. *FEBS Lett* 583:607–614. <https://doi.org/10.1016/j.febslet.2009.01.023>.
48. Douglas GW. 1962. The Glenfield strain of myxoma virus. Its use in Victoria. *J Agric (Victoria)* 60:511–516.
49. Samal A, Schormann N, Cook WJ, DeLucas LJ, Chattopadhyay D. 2007. Structures of vaccinia virus dUTPase and its nucleotide complexes. *Acta Crystallogr D Biol Crystallogr* 63:571–580. <https://doi.org/10.1107/S0907444907007871>.
50. De Silva FS, Moss B. 2008. Effects of vaccinia virus uracil DNA glycosylase catalytic site and deoxyuridine triphosphatase deletion mutations individually and together on replication in active and quiescent cells and pathogenesis in mice. *Virol J* 5:145. <https://doi.org/10.1186/1743-422X-5-145>.
51. Pritchard MN, Kern ER, Quenelle DC, Keith KA, Moyer RW, Turner PC. 2008. Vaccinia virus lacking the deoxyuridine triphosphatase gene (F2L) replicates well in vitro and vivo but is hypersensitive to the antiviral drug (N)-methanocarboxamide. *Virol J* 5:39. <https://doi.org/10.1186/1743-422X-5-39>.
52. Ariza M-E, Glaser R, Kaumayer PTP, Jones C, Williams MV. 2009. The EBV-encoded dUTPase activates NF-κB through the TLR2 and MyD88-dependent signaling pathway. *J Immunol* 182:851–859. <https://doi.org/10.4049/jimmunol.182.2.851>.
53. Mansouri M, Barteel E, Gouveia K, Hovey Nerenberg BT, Barrett J, Thomas L, Thomas G, McFadden G, Früh K. 2003. The PHD/LAP-domain protein M153R of myxoma virus is a ubiquitin ligase that induces the rapid internalization and lysosomal destruction of CD4. *J Virol* 77:1427–1440. <https://doi.org/10.1128/JVI.77.2.1427-1440.2003>.
54. Barteel E, McCormack A, Früh H. 2006. Quantitative membrane proteomics reveals new cellular targets of viral immune modulators. *PLoS Pathog* 2:e107. <https://doi.org/10.1371/journal.ppat.0020107>.
55. Collin N, Guérin J-L, Drexler I, Blanié S, Gelfi J, Boullier S, Foucras G, Sutter G, Messud-Petit F. 2005. The poxviral scrapin MV-LAP requires a myxoma

- viral infection context to efficiently downregulate MHC-I molecules. *Virology* 343:171–178. <https://doi.org/10.1016/j.virol.2005.07.032>.
56. Ramelot TA, Cort JR, Yee AA, Liu F, Goshe MB, Edwards AM, Smith RD, Arrowsmith CH, Dever TE, Keenedy MA. 2002. Myxoma virus immunomodulatory protein M156R is a structural mimic of eukaryotic translation initiation factor eIF2 $\alpha$ . *J Mol Biol* 322:943–954. [https://doi.org/10.1016/S0022-2836\(02\)00858-6](https://doi.org/10.1016/S0022-2836(02)00858-6).
  57. Elde NC, Child SJ, Eickbush MT, Kitzman JO, Rogers KS, Shendure J, Geballe AP, Malik HS. 2012. Poxviruses deploy genomic accordians to adapt rapidly against host antiviral defenses. *Cell* 150:831–841. <https://doi.org/10.1016/j.cell.2012.05.049>.
  58. Manes NP, Estep RD, Mottaz HM, Moore RJ, Claus TRW, Monroe ME, Du X, Adkins JN, Wong SW, Smith RD. 2008. Comparative proteomics of human monkeypox and vaccinia intracellular mature and extracellular enveloped virions. *J Proteome Res* 7:960–968. <https://doi.org/10.1021/pr070432+>.
  59. Doellinger J, Schaade L, Nitsche A. 2015. Comparison of the cowpox virus and vaccinia virus mature virion proteome: analysis of the species- and strain-specific proteome. *PLoS One* 10:e0141527. <https://doi.org/10.1371/journal.pone.0141527>.
  60. Zachertowska A, Brewer D, Evans DH. 2006. Characterization of the major capsid proteins of myxoma virus particles using MALDI-TOF mass spectrometry. *J Virol Methods* 132:1–12. <https://doi.org/10.1016/j.jviromet.2005.08.015>.
  61. Van Vliet K, Momhamed RM, Zhang L, Villa NY, Werden SJ, Lin J, McFadden G. 2009. Poxvirus proteomics and virus-host protein interactions. *Microbiol Mol Biol Rev* 73:730–749. <https://doi.org/10.1128/MMBR.00026-09>.
  62. Alzhanova D, Hammarlund E, Reed J, Meermeier E, Rawlings S, Ray CA, Edwards DM, Bimber B, Legasse A, Planer S, Sprague J, Axthelm MK, Pickup DJ, Lewinsohn DM, Gold MC, Wong SW, Sacha JB, Slifka MK, Früh K. 2014. T cell inactivation by poxviral B22 family proteins increases viral virulence. *PLoS Pathog* 10:e1004123. <https://doi.org/10.1371/journal.ppat.1004123>.
  63. Kerr PJ, Perkins HD, Inglis B, Stagg R, McLaughlin E, Collins SV, van Leeuwen BH. 2004. Expression of rabbit IL-4 by recombinant myxoma viruses enhances virulence and overcomes genetic resistance to myxomatosis. *Virology* 324:117–128. <https://doi.org/10.1016/j.virol.2004.02.031>.
  64. Kerr PJ, Rogers MB, Fitch A, Depasse JV, Cattadori IM, Hudson PJ, Tschärke DC, Holmes EC, Ghedin E. 2013. Comparative analysis of the complete genome sequence of the California MSW strain of myxoma virus reveals potential host adaptations. *J Virol* 87:12080–12089. <https://doi.org/10.1128/JVI.01923-13>.
  65. Chakrabarti S, Sisler JR, Moss B. 1997. Compact, synthetic, vaccinia virus early/late promoter for protein expression. *Biotechniques* 23:1094–1097.
  66. Wong YC, Lin LC, Melo-Silva CR, Smith SA, Tschärke DC. 2011. Engineering recombinant poxviruses using a compact GFP-blasticidin resistance fusion gene for selection. *J Virol Methods* 171:295–298. <https://doi.org/10.1016/j.jviromet.2010.11.003>.
  67. Liu J, Kerr PJ. 2016. Myxoma virus, p 855–867. *In* Liu D (ed), *Molecular detection of animal viral pathogens*. CRC Press, Boca Raton, FL.
  68. National Research Council. 2011. *Guide for the care and use of laboratory animals*, 8th ed. National Academies Press, Washington, DC.